FUEL CELL COOLING SYSTEM DESIGN FOR HYDROGEN-POWERED CONCEPT AIRCRAFT

F. Quaium¹, T. Bielsky^{1*}, F. Thielecke¹

¹ Hamburg University of Technology, Institute of Aircraft Systems Engineering, Nesspriel 5, 21129 Hamburg, Germany

* Corresponding Author

Abstract

The integration of hydrogen as an energy source and fuel cell systems as power sources in disruptive aircraft concepts introduces new challenges for on-board systems design. One such challenge is the heat management of low-temperature proton-exchange membrane fuel cells, which have an average efficiency of around 50%. Although this efficiency is higher than conventional propulsion technologies like gas turbines, these fuel cells operate at a relatively low temperature, between 60 °C and 90 °C, requiring an active cooling system. This paper presents the design of a cooling system for this fuel cell technology integrated into a hydrogen-powered regional concept aircraft with ten propulsion units based on a potential analysis. Different baseline cooling system layouts are evaluated, analyzing both one-phase and two-phase cooling fluids, along with potential synergy effects with other systems. For example, hydrogen can be used as a heat sink in addition to the air from ram air channels. These architectures are assessed based on systems mass and their influence at the aircraft level, taking into account additional drag from the ram air and the electric power requirements of the cooling system. The results show that for cooling system with ram air as single heat sink, the system mass can be decreased by 43 % when using a two-phase cooling fluid instead of a one-phase cooling fluid. Additionally, on system level, the mass of a cooling system with ram air as single heat sink is significantly lower than a cooling system that uses hydrogen as an additional heat sink. However, on aircraft level, the electric power required for hydrogen conditioning needs to be taken into account as well because the hydrogen needs to be conditioned fully electrically for the single-sink architecture.

Keywords

Aircraft Cooling System; Fuel Cell System; Liquid Hydrogen; Overall Systems Design

1

1. INTRODUCTION

Hydrogen is considered a potential energy source to significantly reduce carbon emissions in the aviation sector [1]. For regional aircraft, hydrogen can be combined with fuel cell systems to power an electric power train [2]. Among fuel cell technologies, lowtemperature proton-exchange membrane fuel cells (LT-PEMFC) are particularly promising due to their high technology readiness level compared to other fuel cell technologies [3]. LT-PEMFC offer an average efficiency of around 50 %, which is superior to conventional propulsion technologies like gas turbines [2]. However, integrating such disruptive technologies in an aircraft introduces new challenges for the design of on-board systems (OBS). Specifically, LT-PEMFC operate at relatively low temperatures, between 60 °C and 90 °C, requiring an active cooling system [4,5]. To address the challenges due to the integration of LT-PEMFC in aircraft, it is essential to evaluate cooling systems architectures, as well as potential synergies and interdependencies with other OBS during the conceptual aircraft design phase. Hence,

the *GeneSys* framework, developed by the Institute of Aircraft Systems Engineering (FST) at Hamburg University of Technology (TUHH), is used for the integration of such disruptive OBS into its physics-based overall systems design (OSD) approach [6,7].

This paper presents baseline concepts for LT-PEMFC cooling systems, using a hydrogen-powered regional concept aircraft as use case. The baseline concepts for the cooling system include the following variations, which are discussed in this paper:

- Varying the cooling fluid for one-phase and twophase operation,
- Combining the fuel cell stacks, components of the electric power train, and the heat generated from compressing the air for the fuel cell stacks as heat sources.
- Integrating hydrogen as an additional heat sink alongside ram air.

Figure 1 illustrates the hydrogen-powered regional concept aircraft *ESBEF Concept Plane 1 (ESBEF-CP1)* [7]. The *ESBEF-CP1* has been developed by the German Aerospace Center (DLR) as part of the



FIG 1. Hydrogen-powered concept aircraft ESBEF-CP1

EXACT project and is derived from an ATR 72-like aircraft model [7]. As shown in fig. 1, the ESBEF-CP1 has ten propulsion units (pods), each containing a hybrid LT-PEMFC system, along with its balance of plant components, which include, among others, hydrogen supply, oxygen supply, and the cooling system. The hydrogen required for the LT-PEMFC is stored in two cryogenic tanks positioned in the aft section of the fuselage. Table 1 outlines the relevant top-level aircraft requirements (TLARs) of the ESBEF-CP1, while fig. 2 shows the total shaft power throughout the design mission trajectory [7].

TAB 1. TLARs of the ESBEF-CP1

Characteristic	Value
Design Range [NM]	1000
Cruise Speed [-]	0.55
Cruise Altitude [ft]	27000
Max. PAX number [-]	70

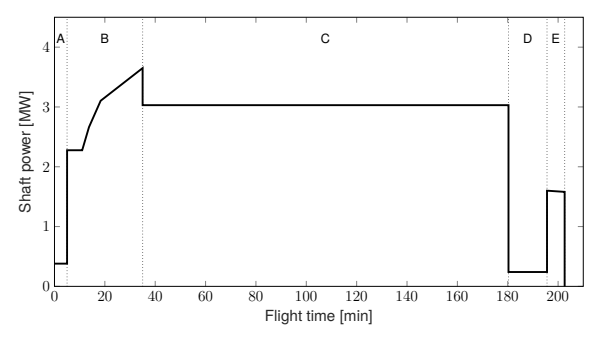


FIG 2. Power profile according to design flight mission (A: Taxi, B: Take-off and Climb, C: Cruise, D: Descent, E: Landing)

The paper is structured as follows. Section 2 introduces the relevant heat sources and heat sinks that serve as boundary conditions for the cooling system of the *ESBEF-CP1*. Based on that, the general parametric sizing approach for the cooling system is presented in section 3. Section 4 describes the OSD framework, which is used as an approach for the parametric sizing of the cooling system. Based on that, concept studies are performed, which are then presented in section 5.

2. INTERFACES TO THE COOLING SYSTEM FOR FUEL CELL-BASED PROPULSION CONCEPTS

The purpose of the cooling system is to transfer heat from heat sources to the heat sinks. In this section, relevant heat sources and heat sinks for the *ESBEF-CP1* pod architecture are introduced.

2.1. Heat sources

As introduced earlier, the primary heat source for the cooling system are the fuel cell stacks in the pods. However, the potential for optimizing the cooling system design is analyzed by including additional heat sources. Figure 3 illustrates the relevant components for electric power flow in a pod, which include the fuel cell stacks and batteries as power sources, the power management and distribution unit (PMAD), the power train for thrust generation, and the connection to supply the OBS. It is assumed that the heat loads from the fuel cell stacks $\dot{Q}_{\rm FC}$ and the power train $\dot{Q}_{\rm ED}$ are relevant for consideration. Among these, the fuel cell stacks generate the highest heat load due to their relatively low efficiency [8]. While the heat loads from the batteries Q_{Bat} are also relevant, they are not considered in this case because the optimal operating temperature of a battery differs significantly from that of the power train or the fuel cell stacks [4,9,10]. Therefore, a separate cooling system needs to be integrated for the battery. Lastly, it is assumed that the heat load from the PMAD can be neglected, as it is not significant compared to the heat loads from the fuel cell stacks and the power train.

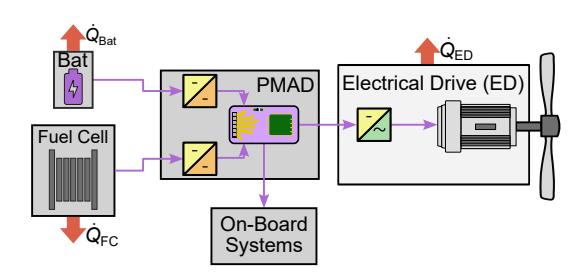


FIG 3. Main heat sources in a hybrid fuel cell-powered propulsion unit

As illustrated in fig. 3, the heat sources generate a thermal flow \dot{Q} . For the fuel cell stacks in each pod, the heat flow $\dot{Q}_{\text{FC,pod}}$ is calculated according to eq. (1) and is dependent on the generated electric power $P_{\text{el.,FC,pod}}$, the cell voltage U_{cell} , which depends on the power values delivered by the fuel cell stacks throughout the mission trajectory, and the thermoneutral cell voltage U_{th} . The value of the thermoneutral cell voltage varies depending on the state of the product water produced by the fuel cell stacks. For a gaseous state, U_{th} is calculated using the lower heating value (LHV) and is $U_{\text{th,LHV}} = 1.253\,\text{V}$ [4, 5]. For a liquid state, the calculation is based on the higher heating value (HHV) and is $U_{\text{th,LHV}} = 1.481\,\text{V}$ [4, 5].

$$\dot{Q}_{\text{FC,pod}} = P_{\text{el.,FC,pod}} \cdot \left(\frac{U_{\text{th}}}{U_{\text{cell}}} - 1 \right)$$

Other thermal flows, such as those from the power train (including the electric motor and its motor controller) or the batteries, are calculated based on their efficiency values. These efficiency values are taken from specific data sheets or calculated with physical simulation models. For instance, the heat flow generated by the electric motor can be calculated using eq. (2) as an example.

(2)
$$\dot{Q}_{\text{motor}} = P_{\text{el.,motor}} \cdot (1 - \eta_{\text{motor}})$$

Furthermore, additional heat sources need to be accounted for in the cooling system. Due to the varying environmental conditions throughout the aircraft's flight envelope, a compressor is necessary to maintain the required pressure for the oxygen supply for the fuel cell stacks. In this case, the losses from the compressor (cf. eqs. (3) and (4)) and the temperature rise of the air during the compression process must be considered. It is assumed that these heat flows are absorbed by the fluid of the cooling system.

(3)
$$\dot{Q}_{\text{air}} = \dot{m}_{\text{air}, \text{FC,pod}} \cdot c_{\text{p}} \cdot (T_{\text{comp,out}} - T_{\text{FC}})$$

(4)
$$\dot{Q}_{\text{comp.air}} = \dot{Q}_{\text{compressor}} + \dot{Q}_{\text{air}}$$

2.2. Heat sinks

Two heat sinks for the cooling system are considered in the scope of this paper: the integration of a ram air channel and the usage of hydrogen.

As shown in fig. 4, the ram air channel for the cooling system consists of an inlet, a diffusor, a heat exchanger (HX), and a nozzle. Additionally, a fan is integrated to facilitate airflow on ground. For the design of the heat exchanger, an isentropic change of states approach is assumed [11]. Through the heat exchanger in the ram air channel, the heat flow $Q_{\text{ram,air}}$ is transferred to the air that passes through the channel. This heat flow is calculated according to eq. (5).

(5)
$$\dot{Q}_{\text{ram,air}} = \dot{m}_{\text{air,FC,pod}} \cdot c_{\text{D}} \cdot \Delta T_{\text{HX}}$$

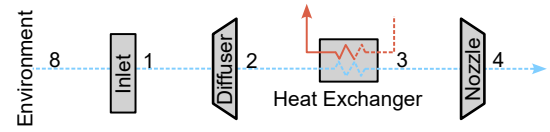


FIG 4. Simplified layout of a ram air channel

Figure 5 illustrates the relevant heat flows in the hydrogen system necessary to heat the hydrogen to the operational conditions required by the fuel cell stacks. For hydrogen storage, the heat flow $\dot{Q}_{\rm env}$ represents the heat transferred from the environment to the cryogenic tank. Additionally, gaseous hydrogen is returned to the tank to maintain the pressure. The heat introduced to the tank from this process is described with $\dot{Q}_{\rm press,cond}$ [12, 13]. $\dot{Q}_{\rm req}$ describes the heat flow inside the tank between the liquid and the gaseous phase to maintain constant pressure.

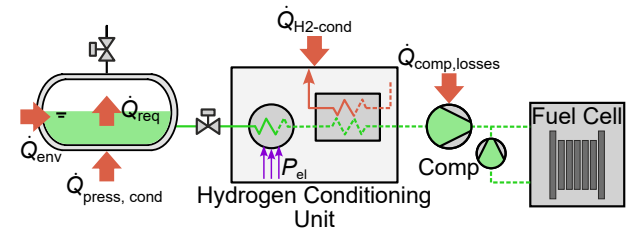


FIG 5. Exemplary illustration of the heat flows on the hydrogen educt side

As part of the hydrogen supply system, the liquid hydrogen must be vaporized and heated to reach the required temperature for fuel cell operation. It is assumed that the vaporization of hydrogen is performed by an electrical heater, while further temperature increases of the gaseous hydrogen can be achieved using a heat exchanger from the cooling system of the fuel cell stacks and is calculated according to eq. (3), using the hydrogen mass flow $\dot{m}_{\rm H2,FC,pod}$, the specific heat capacity depending on the hydrogen's temperature $c_{\rm p}(T)$, and the temperature difference $\Delta T_{\rm H2.HX}$ between the hydrogen entering the fuel cell to the initial temperature of the hydrogen entering the heat exchanger. The heat flow associated with the conditioning of hydrogen as part of the supply system is described as $Q_{\rm H2-cond}$.

For the fuel cell stacks, a compressor-based feed is employed to supply hydrogen at a constant pressure. Consequently, it is assumed that the heat from the compressor losses $\dot{Q}_{\rm comp,losses}$ is transferred to the hydrogen.

3. PARAMETRIC DESIGN OF THE COOLING SYSTEM FOR FUEL CELL SYSTEM PROPULSION

The cooling of a fuel cell stack can be accomplished using air up to a maximum power level of $5\,\mathrm{kW}.$ However, as shown in fig. 2, the total required power for the <code>ESBEF-CP1</code> reaches up to $4\,\mathrm{MW}$ when considering losses in the electric power train and the power required for the balance of plant components. Consequently, the fuel cell system in each pod must provide electric power of up to $400\,\mathrm{kW},$ necessitating a liquid cooling system [14–16].

Relevant components of such a liquid cooling system include:

- · Heat sources (fuel cells, power train)
- · Cooling fluid
- Tank

- Distribution system (pipes)
- Components for distribution (pumps, valves)
- · Heat exchanger
- · Heat sinks (e.g., ram air)

The main evaluation criteria for sizing the cooling system are mass, electric power requirements, and the induced drag when using the ram air channel as a heat sink. In the following, the sizing of the relevant components of the cooling system is described, followed by an elaboration on the overall sizing of the cooling system itself.

3.1. Sizing of relevant components

The mass of the **heat exchanger** $m_{\rm HX}$ is calculated using eq. (6), which considers a specific mass factor of $k_{\rm HX}=0.35\,{\rm kW/kg}$ and the heat flow \dot{Q} [17].

$$(6) m_{\rm HX} = k_{\rm HX} \cdot \dot{Q}$$

The mass of the **pump** m_{pump} (cf. eq. (10)) depends on the required electric power $P_{\mathrm{el.,pump}}$, which is calculated using eq. (7). The calculation of $P_{\mathrm{el.,pump}}$ is based on several parameters, including volumetric flow rate of the cooling fluid \dot{V}_{fluid} , the efficiency of the pump η_{pump} , and the total pressure drop of the cooling circuit Δp_{pod} . The volumetric flow rate is calculated using eq. (8) and depends on the heat flow \dot{Q} , the specific heat capacity of the cooling fluid $c_{\mathrm{p,fluid}}$, the density of the fluid ρ_{fluid} , and the temperature difference at the heat sinks ΔT_{HX} .

(7)
$$P_{\rm el.,pump} = \frac{\dot{V}_{\rm fluid}}{\eta_{\rm pump}} \cdot \Delta p$$

(8)
$$\dot{V}_{\mathrm{fluid}} = \frac{\dot{m}_{\mathrm{fluid}}}{\rho_{\mathrm{fluid}}} = \frac{\dot{Q}}{\rho_{\mathrm{fluid}} \cdot c_{\mathrm{p,fluid}} \cdot \Delta T_{\mathrm{HX}}}$$

The total pressure drop is calculated using eq. (9) and represents the sum of the pressure losses within the cooling system. The relevant parameters contributing to this total pressure drop include the pressure loss for the fuel cell stack cooling $\Delta p_{\rm FC}$, for the electric power train cooling $\Delta p_{\rm ED}$, for the heat exchanger at the heat sink $\Delta p_{\rm HX}$, for the pipes $\Delta p_{\rm pipe}$, and for the miscellaneous components such as valves $\Delta p_{\rm misc}$.

(9)
$$\Delta p_{\text{pod}} = \Delta p_{\text{FC}} + \Delta p_{\text{ED}} + \Delta p_{\text{HX}} + \Delta p_{\text{pipe}} + \Delta p_{\text{misc}}$$

The pressure loss in the fuel cell stacks is determined using an experimental approach proposed by VREDDENBORG [16]. The geometric assumptions of the cooling channels are based on the work of Chen [18]. Within the preliminary design framework, it is assumed that scaling the cooling performance can be achieved by increasing the number of additional cooling channels in each fuel cell stack. Flow properties, such as fluid velocity and Reynolds num-

ber, are analyzed to calculate the friction coefficient, taking the law of mass conservation into account. The pressure losses associated with the components of the electric power train are calculated and validated using data from various manufacturers [8].

Subsequently, the mass of the pump can be derived from a databases provided by manufacturers, as indicated in eq. (10) [19].

(10)
$$m_{\text{pump}} = 0.0308 \cdot P_{\text{el.,pump}} + 1.1912$$

The mass of the **fan** in the ram air channel, which generates the necessary mass flow on ground, is calculated using eq. (7). Additionally, the fan mass is determined from the manufacturer's data according to eq. (11), and it depends on the air mass flow required to dissipate energy in the form of heat [20].

$$(11) m_{\text{fan}} = 0.4386 \cdot \dot{m}_{\text{air}} + 0.1104$$

The mass of the **tank** $m_{\rm tank}$, which serves as coolant storage, is determined by estimating the storage geometry using the calculation norm AD 2000 and the material properties of Al2219 (cf. eq. (14)). To calculate the minimum thickness of the tank s_{\min} , as shown in eq. (13), the diameter d_{tank} , the maximum pressure $p_{\rm tank}$, the given material parameter σ , and a safety factor S must be determined. The tank pressure $p_{\rm tank}$ is estimated by summing the atmospheric pressure at ground level with the hydrodynamic pressure resulting from the tank's filling level $h_{\rm fill}$ (cf. eq. (12)). The filling level h_{fill} and the tank diameter d_{tank} are derived from the volume of the tank, which is calculated as the sum of the total fluid volume in the pipes and components, assuming that 30% of the total fluid volume of the cooling circuit is stored in the tank.

$$(12) p_{\mathsf{tank}} = p_{\mathsf{0}} + \rho \cdot g \cdot h_{\mathsf{fill}}$$

$$s_{\min} = \frac{p_{\text{tank}} \cdot d_{\text{tank}}}{2 \cdot \frac{\sigma_{\text{Al2219}}}{S}}$$

(14)
$$m_{\mathsf{tank}} = V_{\mathsf{shell}} \cdot \rho_{\mathsf{Al2219}}$$

In addition to the main components described above, other miscellaneous components, such as separators and valves, are considered depending on the architecture variants. The determination of their masses is also derived from the manufacturer's specifications and depends on the volumetric flow $\dot{V}_{\rm fluid}$ of the cooling fluid, particularly for the separators and throttle valves (cf. eq. (15), eq. (16)) [21, 22]. The mass of the three-way valves is estimated at $1.5\,{\rm kg/valve}$ [23].

(15)
$$m_{\text{valve,throttle}} = 19.481 \cdot \dot{V}_{\text{fluid}}^2 + 7.6117 \cdot \dot{V}_{\text{fluid}} + 0.1487$$

(16)
$$m_{\text{seperator}} = 13.042 \cdot \dot{V}_{\text{fluid}}^2 + 6.4537 \cdot \dot{V}_{\text{fluid}} + 0.8957$$

3.2. System Sizing

To determine the total mass of the cooling system in one pod, the sum of the total component mass $m_{\rm components,pod}$ and the total amount of fluid $m_{\rm fluid,pod}$ in one cooling circuit is calculated, as shown in eq. (17). The total mass of the components includes the mass of the heat exchanger, pump, tank, miscellaneous components, and pipes, calculated based on material and geometrical parameters. Additionally, a factor of 15 % is included to account for mounting elements.

(17)
$$m_{\text{coolingSystem,pod}} = m_{\text{components,pod}} + m_{\text{fluid,pod}}$$

In addition to the evaluation criteria of mass and electric power demand of the cooling circuit at the system level, the evaluation of the induced drag based on the required cooling air mass flow is also relevant for evaluation at the aircraft level. It is assumed, as a worst-case scenario, that the air in the ram air channel is completely decelerated ($v_{\rm out}=0$) [24]. Equation (18) shows the calculation of the maximum drag $W_{\rm max}$ depending on the air mass flow $\dot{m}_{\rm air}$ and the entry velocity of the air $v_{\rm in}$.

(18)
$$W_{\text{max}} = \dot{m}_{\text{air}} \cdot (v_{\text{in}} - v_{\text{out}})$$

For evaluating the impact of the cooling system at the aircraft level, the additional fuel demand is determined based on the approach by PRATT [25], considering the individual effects due to induced drag, electric power required by the pumps, and system mass. To calculate the additional fuel mass for the ESBEF-CP1, a conversion factor of $0.025577\,\mathrm{kg/MJ}$ is derived based on the aircraft's TLARs (cf. table 1) [7,25].

4. OVERALL SYSTEMS DESIGN FRAMEWORK

During the conceptual design phase, the fidelity of OBS models increases throughout the design process. As shown in fig. 6, the design process includes several stages: overall aircraft design (OAD), OSD, and detailed systems design (DSD) [7].

The first step of the aircraft conceptual design process is performed at the OAD level and includes defining the top-level aircraft requirements (TLARs), the geometry of the aircraft model, and a design mission trajectory [7]. Furthermore, the mass of the OBS is initially estimated using regression functions and statistical methods [26].

In contrast to the top-down approach at the OAD level, OBS need to be physically designed and tested for integration into a new aircraft model. This step is performed at the DSD level. Hence, system behavior

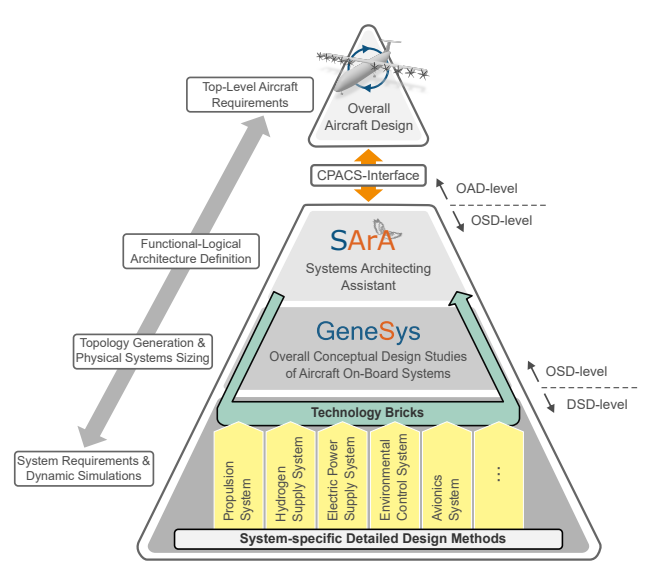


FIG 6. Different stages of conceptual aircraft design from the perspective of a system engineer

analysis based on transient simulations must be conducted to validate requirements for the OBS. High-fidelity and time-dependent simulation models are required, which, however, is a time-consuming process that limits the solution space for system design to a few variants. Additionally, detailed system requirements are not provided by the OAD phase [26].

Both the assessment and selection of feasible system variants, as well as the missing requirements data, are obtained through systems architecting and OSD, respectively. Systems architectures are defined and assessed at the architecture level, while rapid concept studies to identify feasible systems designs and technologies are performed at the OSD level (cf. fig. 6). The Common Parametric Aircraft Configuration Schema (CPACS), defined by the DLR [27], provides an interface file between OAD and other design disciplines during the conceptual design phase.

Applying *GeneSys* to hydrogen-based concept aircraft models necessitates enhancements of the methodology. This is because hybrid fuel cell systems and their balance of plant components (e.g., hydrogen supply and cooling) are integrated into the systems architecture. To this end, the method for overall systems design is in the scope of this paper as an initial integration for the parametric design approach of the cooling system. In the following, concept studies are conducted to identify feasible system architectures while considering the interdependencies between these systems and other OBS. This assessment also includes an evaluation on the aircraft level using key performance indicators such as mass, drag, and the amount of hydrogen required as energy source.

5. SYSTEM ARCHITECTURE STUDIES

Based on the sizing method for the cooling system and the OSD framework introduced above, this sec-

tion presents concept studies focusing on various architecture variants for the cooling system.

5.1. Problem set-up

Two studies are conducted in this section. In the first study, the cooling fluid is varied to analyze both one-phase and two-phase operations, using a single heat source (fuel cell stacks) and a single heat sink (ram air) within the cooling cycle. In the second study, the electric power train and the heat generated from the air compressors are added as additional heat sources to the cooling cycle. Also, operations with and without using hydrogen as a further heat sink are discussed in scope of this study. The evaluation criteria for both studies include system mass, electric power demand, induced drag, and the additional demand of hydrogen as fuel.

5.1.1. System requirements

For the system design of the LT-PEMFC, performance characteristics of the *PowerCell S3* are referenced [29]. The maximum operating temperature is set at $90\,^{\circ}\mathrm{C}$, with a limited maximum temperature difference across the fuel cell stacks of $10\,^{\circ}\mathrm{C}$ and an operating pressure of $2\pm0.9\,\mathrm{bar}$ [5]. The maximum coolant outlet pressure at the fuel cell stack should not exceed $2.4\,\mathrm{bar}$ [29]. To ensure robust operating behavior, stoichiometric factors for the cathode ($\lambda_{O_2}=2$) and anode side ($\lambda_{H_2}=1.15$) are selected [30]. Additionally, it is assumed that the product water in the exhaust is in gaseous state [16]. For the components in the power train, a maximum operating temperature of $80\,^{\circ}\mathrm{C}$ is assumed.

The heat loads of the fuel cell stacks and the power train in one pod over the design flight trajectory are visualized in fig. 7.

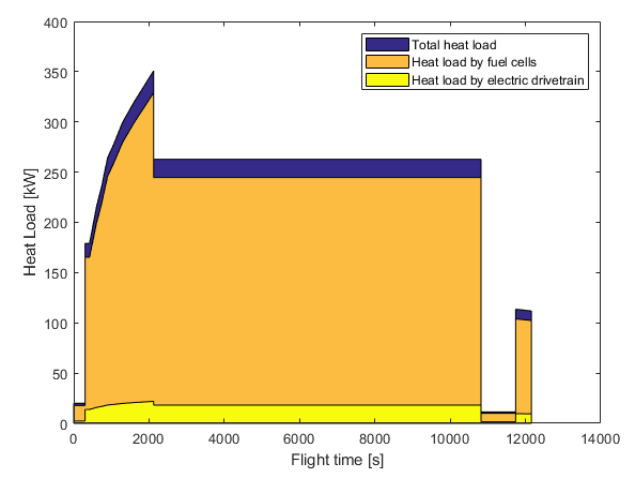


FIG 7. Heat loads of propulsion unit over the flight envelope

Furthermore, it is assumed that the fluid in the pumps operates solely in liquid form, while the compressors handle the fluid entirely in gaseous form [16,31]. Additionally, when using evaporative cooling, the cooling

fluid must enter the fuel cell stack in an undercooled state to mitigate the risk of early evaporation, which could lead to local overheating. In determining the temperatures on the cold side, the waste heat flows from the pump are considered as well, allowing for the calculation of the total degree of subcooling.

5.1.2. Definition of a baseline architecture

As the baseline architecture, a cooling circuit with one heat source (fuel cell stacks) and one heat sink (ram air) is introduced, as illustrated in fig. 8. This setup is designed to analyze the principles of thermal transfer from the heat source to the heat sink. For this baseline architecture, deionized water is selected as cooling fluid for one-phase operation.

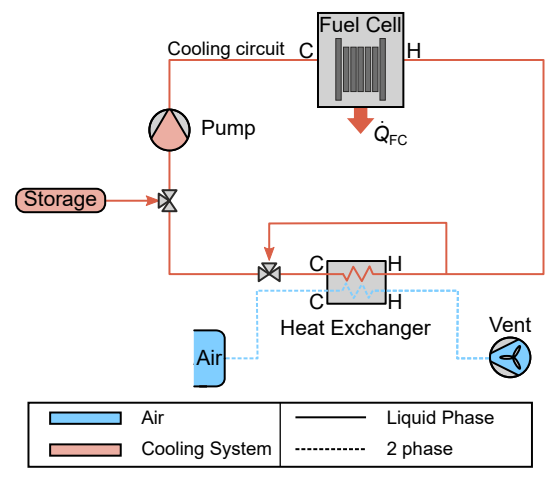


FIG 8. Baseline architecture for the cooling of fuel cell stacks (one-phase)

The baseline architecture includes, in addition to the heat source and heat sink, a tank for storing the cooling fluid and a pump. Furthermore, the cooling fluid can also pass by the heat exchanger of the ram air channel, allowing to control the maximum temperature decrease within the heat exchanger.

5.2. Study 1: Cooling fluid variation

In the context of thermal energy transfer, a distinction is made between sensible heat transfer and latent heat transfer, which occurs through the phase change of the cooling fluid. As previously described, deionized water is selected for the baseline architecture, designed for one-phase operation. In a subsequent step, this fluid is replaced with methanol, which evaporates at the operating pressure and temperature of the fuel cell stack, allowing for two-phase operation. To prevent local overheating of the fuel cell stack due to inadequate contact with the refrigerant, a steam content of $10\,\%$ is selected. For the architecture of the cooling system, it is assumed for simplification that the system components are the same for one-phase and two-phase operation.

Figures 9 and 10 illustrate the total system mass of the baseline system architecture for one-phase and two-phase operations, respectively. The evaluation of system mass clearly indicates a mass improvement when using a cooling fluid that undergoes phase change within the cycle because the mass of the heat exchanger is significantly smaller for two-phase operation. In both architectural variants, the mass of the cooling fluid and the heat exchanger significantly contribute to the overall mass of the system. Additionally, it can be observed that the mass of the pump increases for the architecture with two-phase operation. This increase is attributed to a higher electric power demand of the pump, resulting from significant flow losses in the pipes.

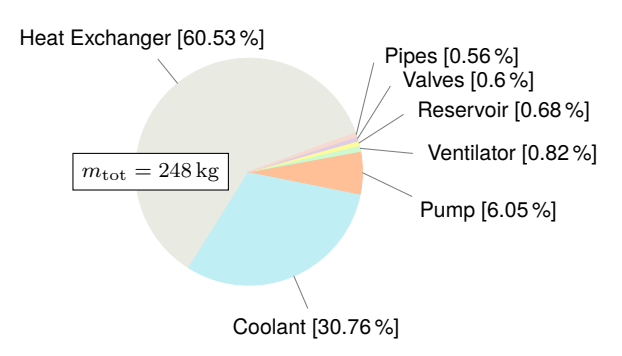


FIG 9. Component mass distribution per pod of the baseline architecture (one-phase)

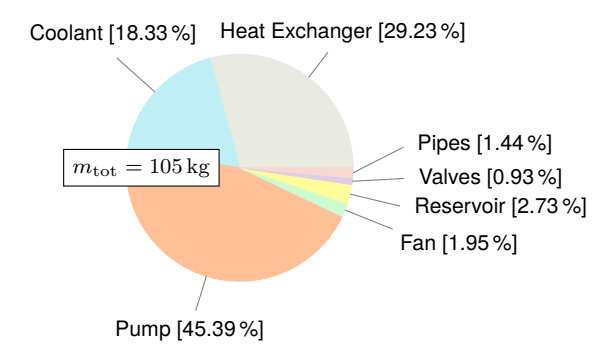


FIG 10. Component mass distribution per pod of the baseline architecture (two-phase)

The evaluation of the baseline architectures for onephase and two-phase operation is shown in fig. 11. The induced drag remains similar for both architectures, as the requirements and boundary conditions of the heat sources and heat sinks are consistent across both designs. When comparing the electric power demand, the architecture with two-phase operation has a slightly higher demand. This increase can be attributed to the increased electric power demand of the pump for two-phase operation, as previously discussed. Lastly, the highest impact on additional fuel consumption is primarily driven by the differences in system mass. The significant reduction in system mass for the two-phase operation architecture due to the smaller heat exchanger results in a corresponding decrease in additional fuel requirements compared to the one-phase operation architecture, even when considering the effect of increased electric power demand.

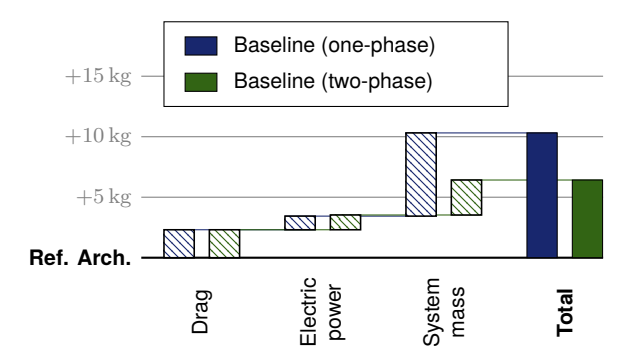


FIG 11. Additional fuel mass (kg_{H_2}) per pod for every considered evaluation metric

5.3. Study 2: Multi-sink operation

In this study, the cooling circuit is enhanced by including the power train heat $(\dot{Q}_{\rm ED})$ and the heat generated from compressing the air $(\dot{Q}_{\rm comp,Air})$ as additional heat sources. Unlike study 1, this analysis focuses exclusively on two-phase operation, using methanol as cooling fluid. Two layouts are compared and evaluated:

- Single-sink architecture: This layout employs ram air as the only heat sink, as illustrated in fig. 12. In this architecture, it is assumed that hydrogen conditioning is performed using electric power only.
- Multi-sink architecture: This design uses both ram air and hydrogen as heat sinks, as shown in fig. 13.
 An electrical heater is still necessary for the hydrogen conditioning process, as it is assumed that the evaporation of hydrogen and partly the temperature increase is performed electrically. Subsequently, the remaining required temperature increase of the hydrogen for entering the fuel cell stack is reached via a heat exchanger connected to the cooling system.

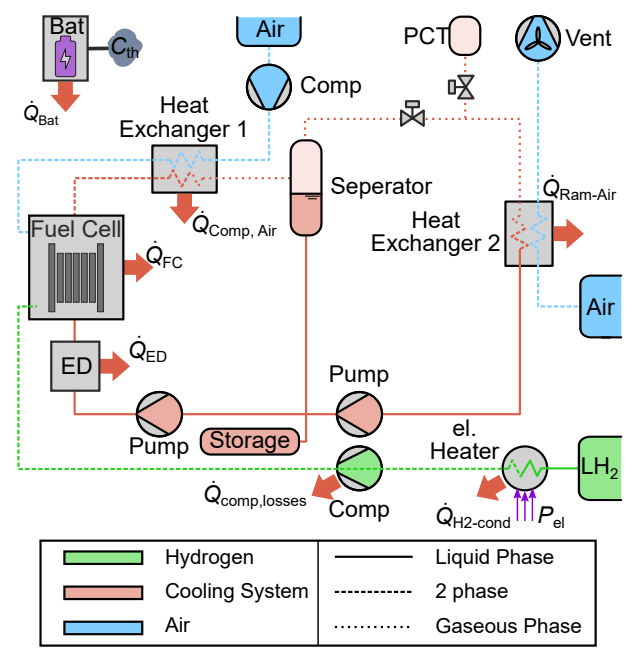


FIG 12. Single-sink architecture (two-phase)

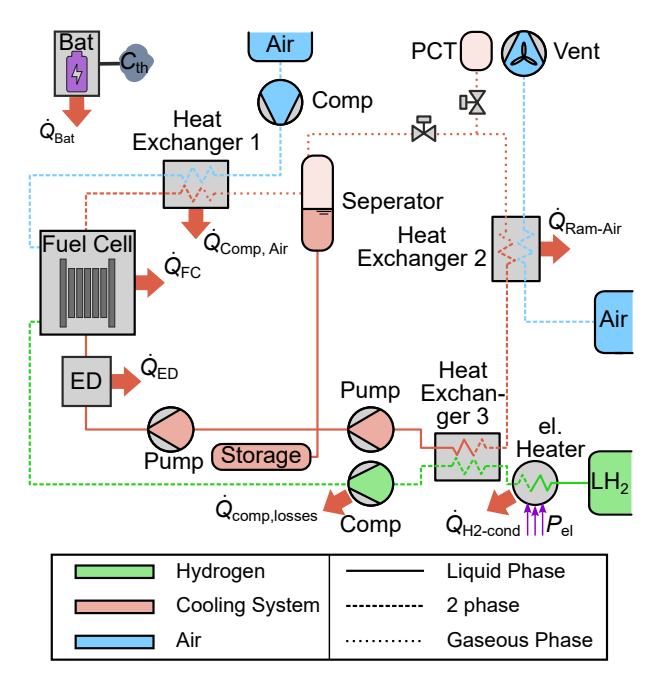


FIG 13. Multi-sink architecture (two-phase)

In both variants, it is assumed that the cooling fluid is fully gaseous after absorbing heat from all three considered heat sources. After passing through the power train, it is assumed that the cooling fluid remains in a liquid state. After passing through the fuel cell stack, the cooling fluid exits in the form of a twophase medium, and after passing through the heat exchanger 1 of the air supply network, it is assumed that the cooling fluid is fully gaseous. A separator ensures that the gaseous and the liquid states of the cooling fluid are kept apart. The cooling fluid is condensed after passing through the heat exchanger 2 in the ram air channel (cf. fig. 12) and further cooled down in case of the multi-sink architecture by the hydrogen in heat exchanger 3 (cf. fig. 13), ensuring that the fluid is fully liquid when it reaches the pumps.

Figures 14 and 15 show the mass of the cooling system architecture with one heat sink and two heat sinks, respectively. It can be seen that the system mass of the multi-sink architecture is significantly higher compared to that of the single-sink architecture. One reason for this increase is the required pipe distance for the coolant from the heat exchanger used for the partial conditioning of the hydrogen to the heat exchanger in the ram air channel. Additionally, more cooling fluid is required for the system.

In fig. 16, the evaluation at the aircraft level is shown. The induced drag is higher for the single-sink architecture because more air is required to pass through the ram air channel to cool the cooling fluid. The electric power demand of the multi-sink architecture is about $11\,\%$ lower compared to that of the single-sink architecture. This reduction is attributed to the decreased air mass flow required in the ram air channel, which is provided by the fans during ground operation, due to the availability of the second heat sink. However, the system mass remains the most relevant factor contributing to the increased additional fuel mass needed

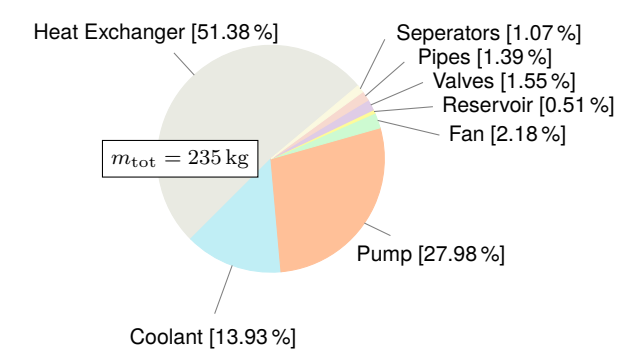


FIG 14. Component mass distribution per pod of the single-sink architecture (two-phase)

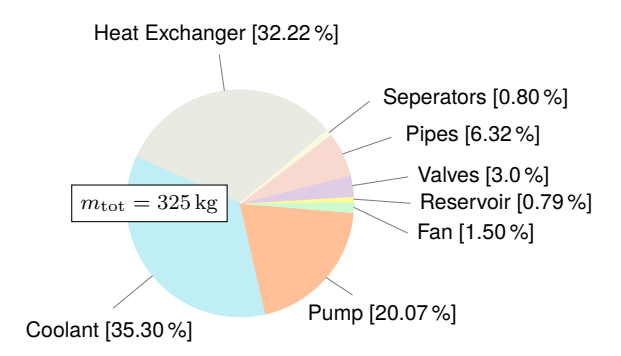


FIG 15. Component mass distribution per pod of the multi-sink architecture (two-phase)

for the multi-sink architecture. Furthermore, at the aircraft level, the required electric power demand for hydrogen conditioning needs to be taken into account. Adding the electric power demand to the evaluation for single-sink and multi-sink cooling system architecture, it is expected that the additional fuel mass of the single-sink architecture is significantly higher than that of the multi-sink architecture.

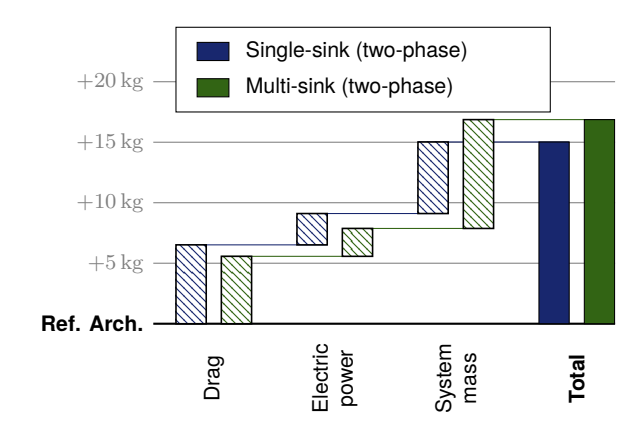


FIG 16. Additional fuel mass (kg_{H_2}) per pod for every considered evaluation metric

6. CONCLUSION AND OUTLOOK

The conceptual design of the cooling system for fuel cell systems as propulsion units in hydrogen-powered concept aircraft is presented in this paper. The use case is a regional concept aircraft with ten propulsion units, each containing a hybrid fuel cell system and an electric power train.

In total, two studies with four architectures of the cooling system are analyzed and evaluated at both the system and aircraft levels. In the first study, a cooling system architecture with a fuel cell stack as the single heat source and a heat exchanger as the single heat sink is introduced as the baseline architecture. The cooling fluid is varied between deionized water for one-phase operation and methanol for two-phase operation. It has been shown that two-phase operation decreases the system mass by $143 \,\mathrm{kg}$ (43 %), thereby also reducing the additional required fuel mass at the aircraft level. In the second study, further heat sources were added to the system: the power train and the heat from the air supply of the fuel cell system. The heat sinks are varied between using only ram air as a heat sink and using both ram air and hydrogen as heat sinks. It has been demonstrated that the mass of the multi-sink architecture is $90 \,\mathrm{kg}$ (38%) higher compared to that of the single-sink architecture. However, these synergy effects for hydrogen conditioning may be necessary, as the power demand for conditioning the hydrogen electrically only may have a more significant impact at the aircraft level compared to using the proposed multi-sink cooling system architecture.

For further studies, the multi-sink architecture needs to be evaluated more thoroughly for assessment at the aircraft level. This means that an optimal and robust design must be established for both the cooling system and the hydrogen conditioning system, leveraging potential synergy effects. Additionally, further evaluation is required to determine whether a multi-source architecture or multiple single-source architectures are more suitable. Finally, the feasibility of a cooling system that uses a cooling fluid in two-phase operation must be further evaluated at the detailed systems design level.

ACKNOWLEDGEMENTS

The results of the presented paper are part of the work in the research project *intelligent Thermal Network (iTherNet)*, which is supported by the Federal Ministry of Economic Affairs and Climate Action in the national LuFo VI program. Any opinions, findings and conclusions expressed in this document are those of the authors and do not necessarily reflect the views of the other project partners.

Supported by:



on the basis of a decision by the German Bundestag

Contact address:

t.bielsky@tuhh.de

References

- [1] Air Transport Action Group. Waypoint 2050: Balancing growth in connectivity with a comprehensive global air transport response to the climate emergency: vision of net-zero aviation by midcentury. 2021.
- [2] Hendrik Schefer, Leon Fauth, Tobias H. Kopp, Regine Mallwitz, Jens Friebe, and Michael Kurrat. Discussion on electric power supply systems for all electric aircraft. *IEEE Access*, Vol. 8:84188–84216, 2020. DOI:10.1109/ACCESS.2020.2991804.
- [3] Horacio R. Corti. Polymer electrolytes for low and high temperature pem electrolyzers. *Current Opinion in Electrochemistry*, 36:101109, 2022. DOI: https://doi.org/10.1016/j.coelec.2022.101109.
- [4] Peter Kurzweil, editor. Brennstoffzellentechnik, 3. Auflage. Springer Fachmedien Wiesbaden GmbH 2016, 2016. ISBN: 978-3-658-14935-2. DOI: 10.1007/978-3-658-14935-2.
- [5] Ryan O'Hayre, Suk-Won Cha, Whitney Colella, and Fritz B. Prinz, editors. Fuel Cell Fundamentals. John Wiley & Sons, 2016. ISBN: 9781119113805. DOI: 10.1002/9781119191766.
- [6] Marc Juenemann, Frank Thielecke, F. Peter, M. Hornung, F. Schültke, and Eike Stumpf. Methodology for design and evaluation of more electric aircraft systems architectures within the avacon project. In *German Aerospace Congress*, Darmstadt, Germany, 2019. DOI: 10.25967/480197.
- [7] Nils Kuelper, Jasmin Broehan, Thimo Bielsky, and Frank Thielecke. Systems architecting assistant (sara) – enabling a seamless process chain from requirements to overall systems design. 33rd Congress of the International Council of the Aeronautical Sciences (ICAS), 2022.
- [8] S. Schaefer, F. Quaium, N. Muhsal, A. Speerforck, F. Thielecke, and C. Becker. Integration of a Cooling System Architecture with a Skin Heat Exchanger for High Thermal Loads in Fuel Cell Powered Aircraft. Herrick Conferences 2022, 2022.
- [9] Bolun Xu, Alexandre Oudalov, Andreas Ulbig, Göran Andersson, and Daniel S. Kirschen. Modeling of lithium-ion battery degradation for cell life assessment. *IEEE Transactions on Smart Grid*, 9(2):1131–1140, 2018. DOI:10.1109/TSG.2016.2578950.

- [10] McKinsey & Company for the Clean Sky 2 JU, Fuel Cells, and Hydrogen 2 JU. Eurocae/sae wg80/ae-7 afc hydrogen fuel cells aircraft fuel cell safety guidelines. *Publications Office of the Eu*ropean Union, 2020. DOI: 10.2843/766989.
- [11] Isabel Pérez-Grande and Teresa J. Leo. Optimization of a commercial aircraft environmental control system. *Applied Thermal Engineering*, 22(17):1885–1904, 2002. DOI: 10.1016/S1359-4311(02)00130-8.
- [12] G. Daniel Brewer. Hydrogen aircraft technology. CRC Press, Boca Raton, 1991. ISBN: 0849358388.
- [13] D. Verstraete. *The Potential of Liquid Hydrogen for long range aircraft propulsion*. Ph. D. Thesis, Cranfield University, November 2021.
- [14] Mark Reichler. Theoretische Untersuchungen zur Kühlleistungssteigerung durch innovative Kühlsysteme für Brennstoffzellen-Elektrofahrzeuge. Dissertation, Universität Stuttgart, Stuttgart, 1.4.2008.
- [15] Guangsheng Zhang and Satish G. Kandlikar. A critical review of cooling techniques in proton exchange membrane fuel cell stacks. *International Journal of Hydrogen Energy*, 37(3):2412–2429, 2012. DOI: 10.1016/j.ijhydene.2011.11.010.
- [16] Enno Vredenborg. Modellbasierter Entwurf von Kühlsystemen für Brennstoffzellen in Verkehrsflugzeugen. Dissertation, 2015.
- [17] U.S. Department of Energy Hydrogen Program. Technical Assessment: Cryo-Compressed Hydrogen Storage for Vehicular Applications.
- [18] F.C. Chen, Z. Gao, R.O. Loutfy, and M. Hecht. Analysis of optimal heat transfer in a pem fuel cell cooling plate. Fuel Cells, 3(4):181–188, 2003. DOI: https://doi.org/10.1002/fuce.200330112.
- [19] EBARA. Ego Circulators: Databook.
- [20] Jeffryes W. Chapman, Sydney L. Schnulo, and Michael P. Nitzsche. Development of a Thermal Management System for Electrified Aircraft.
- [21] Parker Hannifin Corporation. Hypersep Serie STH & SFH: Zyklon Wasserabscheider.
- [22] Emerson. AVENTICS: Serie 344, säurebeständig.
- [23] Oventrop. "Tri-CTR" Dreiwege-Verteil- und Mischventile flachdichtend -: Datenblatt.
- [24] Luca Piancastelli, Leonardo Frizziero, and G. Donnici. The meredith ramjet: An efficient way to recover the heat wasted in piston engine cooling. ARPN Journal of Engineering and Applied Sciences, 10:5327–5333, 2015.

- [25] Joseph W. Pratt, Leonard E. Klebanoff, Karina Munoz-Ramos, Abbas A. Akhil, Dita B. Curgus, and Benjamin L. Schenkman. Proton exchange membrane fuel cells for electrical power generation on-board commercial airplanes. *Applied Energy*, 101:776–796, 2013. DOI: 10.1016/j.apenergy.2012.08.003.
- [26] Thimo Bielsky, Marc Juenemann, and Frank Thielecke. Parametric modeling of the aircraft electrical supply system for overall conceptual systems design. In *German Aerospace Congress*, Bremen, Germany, 2021.
- [27] Marko Alder, Erwin Moerland, Jonas Jepsen, and Björn Nagel. Recent advances in establishing a common language for aircraft design with cpacs. In *Aerospace Europe Conference*, Bordeaux, France, 2020.
- [28] Marc Juenemann, Vivian Kriewall, Thimo Bielsky, and Frank Thielecke. Overall systems design method for evaluation of electro-hydraulic power supply concepts for modern mid-range aircraft. In AIAA AVIATION 2022 Forum, Chicago, USA, 2022. DOI: 10.2514/6.2022-3953.
- [29] PowerCell. Powercellution p stack. https://www.datocms-assets.com/36080/1636022110-p-stack-v-221.pdf.
- [30] Helmut Löhns. Leistungsvergleich von Nieder- und HochtemperaturPolymerelektrolytmembran-Brennstoffzellen
 Experimentelle Untersuchungen, Modellierung
 und numerische Simulation. Dissertation,
 Technischen Universität Darmstadt, Darmstadt,
 23.08.2010.
- [31] Weibo Chen, David W. Fogg, Michael Izenson, and Cable Kurwitz. A Highly Stable Two-Phase Thermal Management System for Aircraft. In SAE Technical Paper Series, SAE Technical Paper Series. SAE International400 Commonwealth Drive, Warrendale, PA, United States, 2012. DOI: 10.4271/2012-01-2186.